Remote Sensing of Environment 125 (2012) 125–133

Contents lists available at SciVerse ScienceDirect

Remote Sensing of Environment

journal homepage: www.elsevier.com/locate/rse

Using LiDAR to quantify topographic and bathymetric details for sea turtle nesting beaches in Florida

Kristina H. Yamamoto [a,*], Rebecca L. Powell [a,b], Sharolyn Anderson [c,d], Paul C. Sutton [a,c,d]

[a] Department of Geography, University of Denver, 2050 East Iliff Ave., Denver, CO 80208, United States
[b] Center for Energy Environment and Sustainability, Department of Biology, Wake Forest University, 1834 Wake Forest Rd., Winston-Salem, NC 27109, United States
[c] School of Natural and Built Environments, University of South Australia, Mawson Lakes, Adelaide, SA, 5001, Australia
[d] Barbara Hardy Institute University of South Australia, Mawson Lakes, Adelaide, SA, 5001, Australia

ARTICLE INFO

Article history:
Received 1 February 2012
Received in revised form 19 July 2012
Accepted 21 July 2012
Available online xxxx

Keywords:
LiDAR
Sea turtle
Habitat model
Coastal
Bathymetry
Topography

ABSTRACT

Sea turtles nesting beaches are found near-globally, and the ability to characterize beaches by topographic and bathymetric features has remained largely out of reach. Twenty-one beaches and their offshore areas in southern Florida used by three sea turtle species (*Caretta caretta*, *Chelonia mydas*, and *Dermochelys coriacea*) were compared using topographic measures derived from LiDAR data. Variables such as slope, aspect, rugosity, and topographic and bathymetric position indices (TPI and BPI) were extracted from the LiDAR surface raster to characterize beaches used by sea turtles; stepwise multiple regression was used to determine which variables are most strongly associated with turtle nesting density. The three species exhibited tolerances for similar ranges of values in measured variables; beaches with values outside these tolerances were not used for nesting. Beach nesting density can be successfully modeled for all three species, but different topographic measures were important in each model. This work demonstrates the potential of high spatial resolution topographic datasets to successfully characterize coastal habitat for ecological applications.

1. Introduction

Many coastal species are at risk due to habitat loss from beach construction and sea level rise. Sea turtles are particularly vulnerable, as all nesting efforts occur on low-lying beaches. Past research efforts, though intensive, have failed to determine exact requirements by different marine turtle species for nesting beaches. In addition, the characteristics of beaches and nesting sites within beaches used in by the seven different species vary globally, and few commonalities appear to exist. Green turtles, *Chelonia mydas*, for example, appear to prefer nesting near or within vegetation, as roots provide structure in nest building (Brown & Macdonald, 1995; Bustard, 1972; Bustard & Greenham, 1968; Chen et al., 2007). Leatherback turtles, *Dermochelys coriacea*, which occasionally nest on the same beaches as green turtles, appear to prefer to nest in the open sand (Whitmore & Dutton, 1985). There is limited research on nesting preferences for other species.

Several biophysical elements that may influence nesting preference have been studied in depth in situ, including sand characteristics, moisture, salinity, beach width and length, amount of vegetation, and temperature (e.g. Bustard & Greenham, 1968; Mortimer, 1990; Stancyk & Ross, 1978). Morphological characteristics of beaches, such as slope and the related offshore approach, have been the addressed in studies, but not to the same extent as the above characteristics. Horrocks and Scott (1991) found that nest elevation above sea level was positively related with hatching success for hawksbill turtles, *Eretmochelys imbricate*. Their study also found that on beaches with less steep slopes, hawksbills nested further from the high tide line, which suggests that hawksbills prefer to nest at a certain mean elevation above sea level, and therefore the females will travel further inland in order to reach the optimum elevation value, even if it means traveling greater distances. Provancha and Ehrhart (1987) reported that segments of beaches with higher slopes had higher nest densities than beaches with lower slopes for loggerhead turtles, *Caretta caretta*. The beaches with the highest slopes, and thus the highest nesting densities, had more gradual drop-offs offshore. The beaches with lower slopes and lower nesting densities had near shore drop-offs bordered by shoals to the one side. The researchers also found that slope and width of nesting beaches were inversely correlated, and that offshore approach may be related to beach slope. As a result of these findings, the researchers suggest that offshore characteristics may influence a sea turtle's choice to nest on a nesting beach.

Mortimer (1982) also hypothesized that slope and offshore configuration of the beach were possibly more important than sand grain properties, although the values were never quantified. However, it is important to note that physical requirements of the different species and even individuals within the same species may determine beach selection. Whitmore and Dutton (1985) suggested that because leatherback turtles are much larger than green turtles, female

* Corresponding author. Tel.: +1 510 316 2656; fax: +1 303 871 2201.
E-mail address: khyamamoto@gmail.com (K.H. Yamamoto).

0034-4257/$ – see front matter © 2012 Elsevier Inc. All rights reserved.
http://dx.doi.org/10.1016/j.rse.2012.07.016

leatherbacks may prefer to nest closer to shore than female green turtles simply due to energy constraints.

Better methods to extract topographic information from coastal areas are a current need in ecological studies. Digital Elevation Models (DEM) are commonly used, due to their relatively low (or no) cost when procured from governmental sources and their widespread geographic availability. However, the spatial and the temporal resolution of DEMs are dependent upon the original data provider, and the spatial resolution in particular can be too coarse for small study areas (e.g., the Shuttle Radar Topography Mission (SRTM) DEM has a spatial resolution of 90 m globally, and 30 m for the United States).

Light Detection and Ranging (LiDAR) data, which uses laser pulses to obtain elevation information, have been used successfully when other commonly used DEMs are not deemed adequate due to their spatial or temporal resolution. Of particular interest to researchers in coastal areas is the ability to quickly highlight small elevational differences across the coastal landscape. Stockdon et al. (2009) utilized LiDAR data to identify dune crests in hurricane-prone areas, which can be used in creating vulnerability maps to aid in disaster planning. Dune erosion from grazing activities can also be quantified with LiDAR (De Stoppelaire et al., 2004), and low-lying areas prone to inundation from sea level rise are more easily identified with LiDAR than other data sources (Gesch, 2009).

Bathymetric features are also possible to visualize using LiDAR with a dual laser system, instead of the single laser used for topographic mapping (Quadros et al., 2008). Aircraft-based LiDAR sensors, in particular, are a more effective method of mapping offshore areas without the need of boat-mounted sonar or laser methods, which can damage shallow water ecosystems (Parson et al., 1997). Collin et al. (2008) used LiDAR to map the shallow water seabed to aid in habitat identification. Also pertaining to off-shore habitat mapping, Zawada and Brock (2009) illustrated that the topographic complexity of coral reefs can be quantified using LiDAR data.

Few studies have compared multiple sea turtle nesting beaches to one another; Mortimer (1990) remains one most often-cited. The lack of studies that compare multiple beaches, topographically and bathymetrically, for multiple species represents a gap in the literature. This gap is largely a result of the time-intensive nature of gathering elevation data in the field, and the difficulty of collecting bathymetric data in general. The relatively recent availability of LiDAR data now enables researchers to conduct elevation-based studies that were previously logistically impossible.

The goals of this research are to investigate the following two questions using LiDAR data and annual turtle nest surveys: (1) Do beaches used by the same species show similar morphological characteristics, and to what degree do these characteristics overlap between species? (2) Can morphological characteristics be used to model sea turtle nesting density? Although the study area will be limited to southeastern Florida, the methods are assumed to be generalizable to other areas of interest.

2. Methods

Beaches were used as the basic spatial unit of analysis in this study, rather than the areas directly surrounding nests. Although the environment in the immediate vicinity of a nest provides insight into why a female chooses to nest at that particular site, and may reveal differences between individuals and within beaches, beach-wide comparisons can highlight similarities and differences across larger geographic areas. In addition, because beaches are used by different species to varying degrees, allowing comparisons at a beach level can potentially highlight a broader range of suitability values for and between species. Finally, data on turtle nesting density were only available at the beach level.

Nesting information was obtained from the Florida Fish and Wildlife Conservation Commission (2008). The data contain the number of nests per beach per year by species, dates of nesting seasons, areas of beach surveyed, and the number of days per week spent surveying. Beaches were included in the current study if monitoring efforts were conducted between 1998 and 2005 with a relatively consistent sampling area and effort. For example, beaches were only included if the surveyed area of a beach varied less than 0.25 km between years and if the number of surveying days conducted per week remained constant between years. In addition, only those beaches with LiDAR coverage within the boundaries for the bathymetric and topographic mapping project by the United States Army Corps of Engineers were considered. On the east coast of Florida, a total of 21 beaches were ultimately included in this study (Table 1, Fig. 1).

Each beach was divided into two areas, onshore (from the inland-most points still classified as beach to the shoreline) and offshore (from the shoreline to a specified point ocean-ward) for analysis. The onshore and offshore areas were used to extract values from the LiDAR-derived rasters, which were then compared across beaches and species. The steps for these processes are detailed below.

LiDAR data were procured from the NOAA Coastal Services Center's Digital Coast website in UTM Zone 17 projection with NAD83 horizontal and NAVD88 vertical datum, LAS 1.1 file format. The data originated from a 2006 topographic and bathymetric mapping project from the United States Army Corps of Engineers and were collected by the Joint Airborne LiDAR Bathymetry Technical Center of Expertise (JALBTCX) using the Compact Hydrographic Airborne Rapid Total Survey (CHARTS) system. LiDAR data collection flights were flown from December 2005 to February 2006, which corresponded to roughly 1 to 2 months after the nesting season of 2005 was completed. The LiDAR flights were typically conducted at low tide (Sylvester, 2011), and the timing of all LiDAR flights allowed for covering summer accretion before winter storm erosion. Vertical accuracy is 0.30 m within two standard deviations, horizontal accuracy is 3.0 m within two standard deviations, and the nominal ground spacing of LiDAR samples is 2.0 m.

The LiDAR cloud data were converted to rasters with varying pixel sizes in order to determine the pixel size that resulted in the best balance between a low percentage of empty cells (i.e. cells with no LiDAR data points) and a minimal amount of data point averaging, which would result in a loss of detail included in the original data. Three sample areas with approximately 400 by 400 m dimensions were chosen from Delray, Golden, and Lantana beaches. For each sample area, LiDAR cloud data were converted to pixels with spatial resolutions varying between 2 and 10 m using the Boise Center Aerospace Laboratory (BCAL) LiDAR toolset, as described in Streutker and

Table 1
List of beaches, and their associated counties and area, included in the study.

Beach Name	County	Area (km^2)
Boca Raton Beaches	Palm Beach	0.390
Deerfield/Hillsboro Beaches	Broward	0.248
Delray Beach	Palm Beach	0.338
Ft Lauderdale Beach	Broward	0.602
Golden Beach	Miami-Dade	0.109
Gulfstream	Palm Beach	0.237
Gulfstream Park	Palm Beach	0.004
Highland Beach	Palm Beach	0.016
Hobe Sound NWR	Martin	0.238
Hollywood/Hallandale Beach	Broward	0.583
John U. Lloyd State Park	Broward	0.267
Jupiter Island	Martin	0.027
Kreusler Park	Palm Beach	0.013
Lake Worth Municipal Beach	Palm Beach	0.017
Lantana	Palm Beach	0.007
Macarthur State Park	Palm Beach	0.003
Ocean Inlet Park	Palm Beach	0.010
Ocean Reef Park	Palm Beach	0.013
Pompano/Lauderdale-by-the-Sea	Broward	0.617
Singer Island	Palm Beach	0.076
Sloan's Curve	Palm Beach	0.050

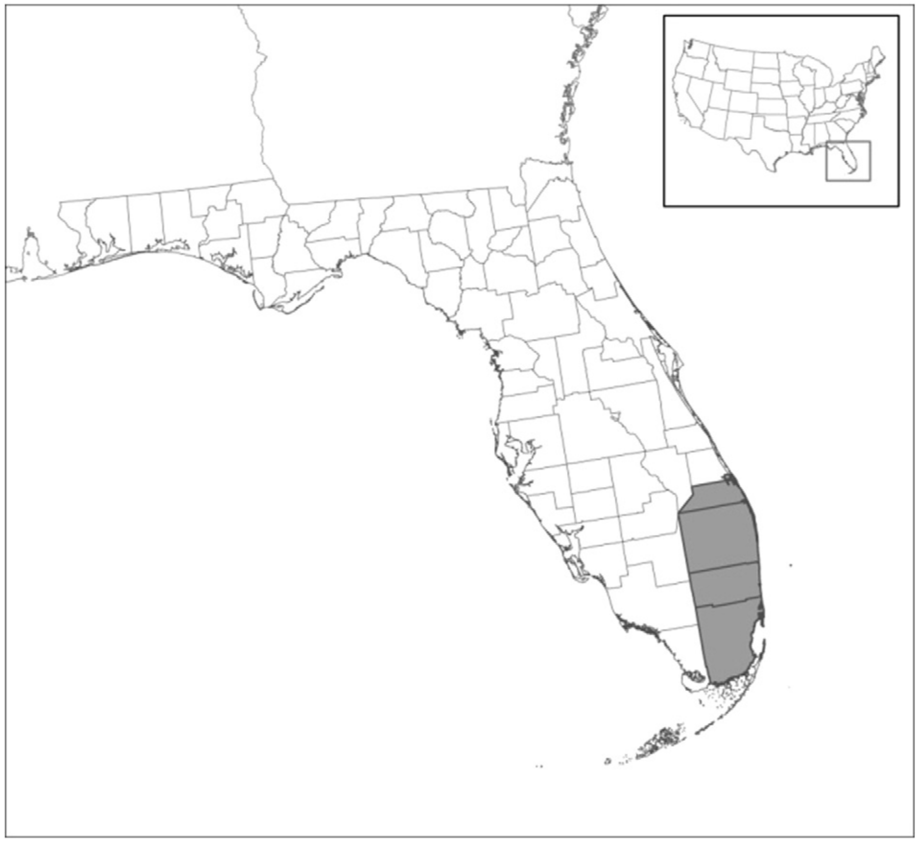

Fig. 1. Counties in Florida with beaches included in the analysis.

Glenn (2006), available as an Exelis Visual Information Solutions ENVI add-on (http://bcal.geology.isu.edulEnvitools.shtml). Points with an elevation of five or more standard deviations from the median value for the dataset were considered outliers and not included in the raster datasets. The percentage of empty cells in each sample area was calculated for each pixel size (Fig. 2). As expected, the percentage of empty cells decreased as the pixel size increased. By the 9 m spatial resolution, there were no empty cells remaining. Based on these results, a pixel size of 5 m for all beaches was chosen for this study, as 5 m resolution minimized empty cells without overly smoothing the original data.

Aside from the expected derived variables, such as mean elevation, slope, aspect, and orientation, two additional variables are commonly calculated to characterize features and highlight changes in elevation across a landscape. Terrain Positional Index (TPI) and the related Bathymetric Position Index (BPI) are derived from slope calculations and illustrate how a pixel in a surface is located relative to other pixels in the raster (Iampietro & Kvitek, 2002; Weiss, 2001). This relative location (i.e. higher or lower than a pixel's neighbors) can be calculated using a number of nearest neighbor algorithms, including the use of circles or rectangles (Lundblad et al., 2006).

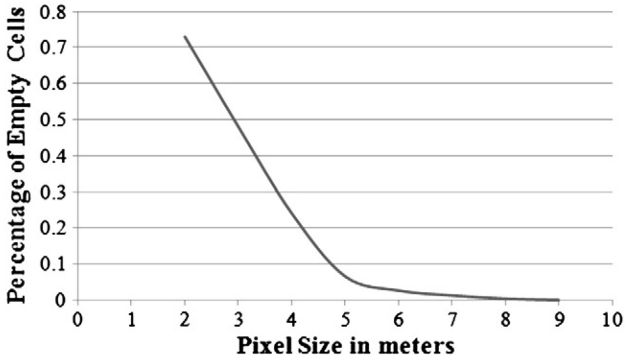

Fig. 2. Percent of no-data cells versus pixel size of raster image generated from LiDAR data (example from Delray Beach, Palm Beach County.).

Surface roughness, or rugosity, is also commonly used in bathymetric studies. Rugosity is defined as the ratio of the surface area to the planar area (Jenness, 2011). Areas with a rugosity value of 1 are flat, indicating no difference between the surface area and the planar area ratio. Areas with rugosity values greater than 1 have some degree of roughness, with higher values indicating a greater degree of roughness. For example, a Himalayan peak will have a higher rugosity value than a cornfield in Iowa representing the same ground area. Rugosity calculated from LiDAR-derived surfaces corresponds well with in-situ measurements for finer spatial resolutions (Wedding et al., 2008).

Depth, slope, TPI/BPI and rugosity are useful in the creation of a benthic classification system of topographic features (Lundblad et al., 2006). On the ecological side, these variables have been used to identify and predict benthic biotopes (Buhl-Mortensen et al., 2009), to identify benthic habitats (Wilson et al., 2007), and create rockfish predictive models (Iampietro et al., 2008). TPI alone has been used to classify topographic features, such as valleys and canyons, (Weiss, 2001), or combined with rugosity to classify seafloor habitats (Iampietro & Kvitek, 2002).

The resulting elevation rasters were used to construct slope rasters, measured in degrees, and TPI/BPI, rugosity, and aspect raster datasets. Although the length and location of the beaches were included in the data provided by the Florida Fish and Wildlife Conservation Commission (FWC), the defining boundaries of the beaches as provided by the FWC did not always match up with the LiDAR data from 2006. As a result, the St Johns River Water Management District (SJRWMD) (2000) dataset was used to delineate the coastal areas for consistency to subset the LiDAR data into beach areas, similar to the methods implemented by Long et al. (2011). This dataset originates from 1:12,000 United States Geological Survey (USGS) color infrared (CIR) digital orthophoto quarter quadrangles (DOQQs) and represents 1999 land use and land cover for Florida as polygons. Due to the differences in dates of data acquisition, the boundaries of beach areas from the SJRWMD were overlaid on the intensity images from the LiDAR data for comparison. In the vast majority of cases, the areas designated as beaches in the SJRWMD dataset could be used to delineate the beaches, as the 1999 demarcations still applied. For those areas that did not match well, the LiDAR data were used to adjust the 1999 boundaries. The transition from sand (beach) to vegetated areas with buildings (non-beach) was relatively easy to identify using the LiDAR intensity surfaces. Piers and other beach structures were not included in the analysis and were removed from the polygons, as they skew the onshore and offshore heights and slope measurements.

Once the onshore delineations were established, the shoreline and the offshore boundaries were generated. As a result from waves breaking on the land, the LiDAR data contained gaps (or no data) at around 0 m elevation mean sea level (MSL). This area of no data, when digitized and overlaid onto Google Earth imagery (date 12/30/2005), corresponded well with the shoreline in the images. Thus, the first no-data pixels in a direction perpendicular to the beach area were designated as the shoreline.

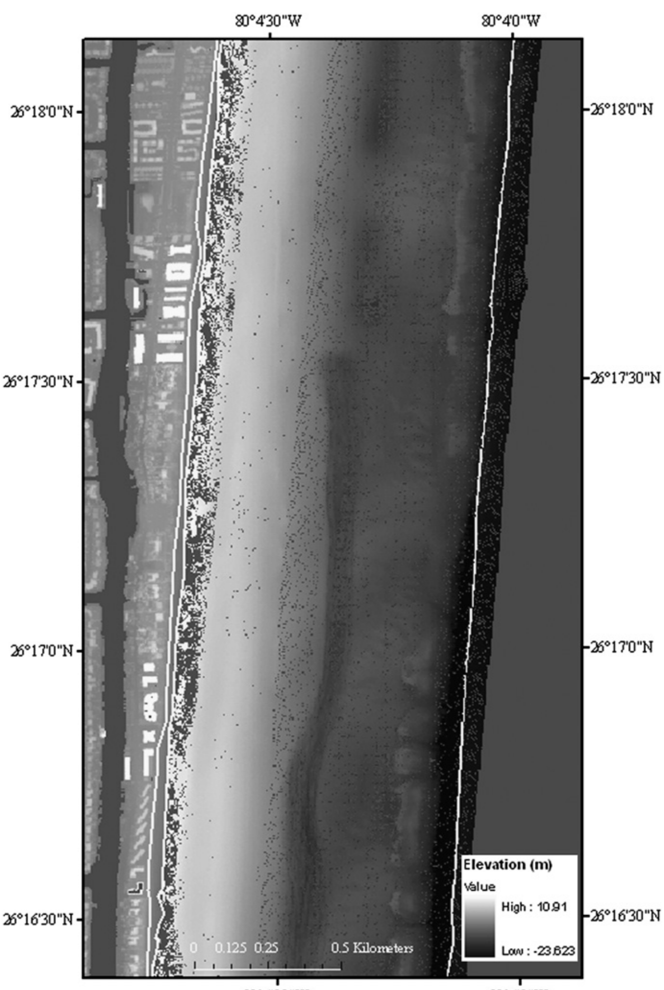

Fig. 3. Example of LiDAR elevation raster with a portion of Deerfield/Hillsboro Beaches represented. The onshore and offshore polygons, shown in white, were used to extract variables from the elevation and elevation-derived raster datasets. The elevation ramp only depicts the range for the raster contained by the polygons.

Table 2
Variables and abbreviated names used in the analysis.

Variable	Measurements
Onshore elevation	Minimum, maximum, mean, standard deviation
Offshore elevation	Minimum, maximum, mean, standard deviation
Onshore slope	Minimum, maximum, mean, standard deviation
Offshore slope	Minimum, maximum, mean, standard deviation
Aspect onshore	Mean, standard deviation
Aspect offshore	Mean, standard deviation
TPI onshore	Minimum, maximum, mean, standard deviation
BPI offshore	Minimum, maximum, mean, standard deviation
Rugosity onshore	Minimum, maximum, mean, standard deviation
Rugosity offshore	Minimum, maximum, mean, standard deviation
Offshore shoals	Area
Beach length	Total
Beach width	Minimum, maximum, mean
Beach orientation	Total

In order to determine the offshore boundaries, the bathymetric dataset was subset to include the area from the shoreline to 1000 m offshore. This distance was chosen to best compare offshore depth and other variables between beaches, because beaches had different widths of offshore areas charted with LiDAR. Although many of the LiDAR datasets contained data far beyond 1000 m, some beaches did not, and using the entire bathymetric dataset would potentially skew the results, as the beaches with data for the farthest distance offshore would likely have the greatest depths.

Thus, for each beach, two polygons represented areas of interest: offshore and onshore (Fig. 3). In addition, rasterized LiDAR intensity surfaces were generated for each beach with elevations for both offshore and onshore areas. These elevation surfaces were used to generate rasters representing slope and aspect for each pixel. TPI/BPI and rugosity raster surfaces were used to further represent surface characteristics. The TPI/BPI grids were created using the CorridorDesigner extension for Esri's ArcMap 9.3 (Majka et al., 2007) with the circle filter and a radius of 4 pixels to capture changes in the landscapes without overly averaging values (4 pixels was chosen as it creates a neighborhood of 20 m from which to determine the TPI/BPI values, which allows for a compromise between small and large neighborhood averaging). Rugosity grids were produced with the DEM Surface Tools for ArcGIS 9.x (Jenness, 2011). The elevation, slope, aspect, TPI/BPI, and rugosity rasters were all clipped to only include the offshore and onshore areas of interest. Other variables, such as orientation (measured in degrees as oriented to the ocean), length, and width of the beach, were recorded. The presence of offshore shoals and their area were also noted, as the presence of shoals has been attributed to lower nesting densities in *C. caretta* (Provancha & Ehrhart, 1987). All of the above measurements were therefore used to extract a number of variables for each beach (Table 2). Because the compass direction orientation and aspect are cyclical variables, they were transformed to their non-cyclical forms for eastness using the sine function (Austin et al., 1990; Piedallu & Gegout, 2008; Pierce et al., 2005).

Similarities between beaches with a similar number of nests per km were evaluated to determine whether beaches with a higher degree of use were characterized by different ranges of morphological variables than beaches with less use. Jenks natural break optimization divisions were applied to the turtle nesting density dataset to assign each beach into one of three classes for each species: high, medium, and low nesting densities. This method divides the data into a predetermined number of classes by minimizing the average deviations from the class mean (Jenks, 1967). These ranks were used to compare beaches of similar nesting use within and between species based on morphological variables.

The variables for each rank were combined. The minimum, maximum, and average of the mean values were calculated for each variable for each rank of the species. Beaches with the highest degree of use for each species were expected to have the narrowest ranges for

Table 3
Jenks divisions for average number of nests per km for each species. The values represent the upper limit for each category.

	Rank low	Rank med	Rank high
C. caretta	76.63	196.05	372.84
C. mydas	9	21.32	62.33
D. coriacea	1.11	3.36	7.19

the most important variables that determine beach use, converging on an "ideal" range for the nesting preferences of that species. Conversely, beaches with less use by a given species were expected to have wider ranges for the important variables, representing the degree to which a beach would be considered suitable for nesting but not able to support larger numbers of nests.

To determine if the beaches with the highest use for each of the species (rank = "high") were characterized by morphologic measures that were statistically different from one another, ANOVA tests were run for offshore and onshore elevation, slope, TPI/BPI, rugosity, and aspect, and beach length, width, and orientation using the mean of the means and the square root of the average of the standard deviations for each variable.

To determine which variables were most strongly associated with turtle nesting density for each species, stepwise multiple linear regression was conducted using SAS Institute Inc.'s JMP Pro 9.0. The average number of nests per kilometer from 1998 to 2005 was used as the response variable. All variables that could potentially be related to nesting activity were originally considered for inclusion in the modeling attempts as the predictor variables. Slope has already been shown to correlate with nesting density (Provancha & Ehrhart, 1987), and elevation with nest location preferences (Horrocks & Scott, 1991). Offshore shoals may also be related to nest density (Provancha & Ehrhart, 1987), and beach orientation, aspect, and length and width measurements provide additional information that may affect beach morphology. While BPI/TPI and rugosity have not been previously used for sea turtle habitat modeling, they have been incorporated into other marine habitat models, such as Iampietro et al. (2008). The minimum, maximum, mean, and standard deviation of slope and elevation, both for onshore and offshore areas, were included, as were offshore shoal and onshore aspect, width, and length measurements.

For rugosity and BPI/TPI, maximum, mean, and standard deviation of values were included; however, offshore mean BPI and offshore and onshore minimum rugosity had values too similar across all beaches to be included in the model. In addition, minimum BPI/TPI measurements were removed from consideration as sea turtles coming ashore to nest may be less affected by the lowest areas than the surroundings, and more affected by the highest peaks and overall landscape surface characteristics. Stepwise multiple regressions were run to determine the best model for each species, with a balance sought between low root-mean-square error (RMSE) and Akaike information criterion (AIC) values, and high adjusted R^2 with a minimum number of variables.

3. Results

3.1. Beach-wide comparisons within and between species

3.1.1. Within species

The Jenks divisions divided the beaches into rankings for average number of nests per km per species (Table 3), and the assigned rank for each beach, and the ranges observed for each variable, are shown in Tables 4 and 5.

Offshore and onshore elevation, slope, TPI/BPI, and rugosity were compared across ranks for each species. Some of the variables demonstrated a clear gradient for each species, with low rank beaches having the greatest variability and the highest ranking beaches having less, such as BPI offshore (Fig. 4). (For *C. caretta*, offshore and onshore BPI/TPI and offshore rugosity showed such gradients; for *C. mydas*, offshore and onshore rugosity and offshore BPI did; none of the variables tested for *D. coriacea* demonstrated such a pattern). The remaining variables showed no distinct trends, such as onshore elevation (Fig. 5).

3.1.2. Between species

Based on the ANOVA tests, none of the variables were statistically different between species at the $p<0.10$ significance level. This indicates that the beaches with the highest use for the three species

Table 4
Beaches and their assigned rank for each species with onshore variables. Minimum and maximum values are reported for elevation, slope, TPI, rugosity, and beach width.

Beach	*C. caretta* use	*C. mydas* use	*D. coriacea* use	Onshore variables								
				Onshore elevation	Onshore slope	Onshore TPI	Onshore rugosity	Onshore aspect	Beach length (km)	Beach width (m)	Sine beach orientation	Sine beach aspect
Boca Raton Beaches	Med	Med	Med	−1.29–6.34	0.04– 34.00	−2.16–2.25	1.00–1.11	102.14	7.60	26.19–83.29	0.16	0.98
Deerfield/Hillsboro Beaches	Med	Med	Med	−1.70–6.38	0.02–24.55	−0.53–0.74	1.00–1.02	98.41	6.90	15.64–80.46	0.13	0.99
Delray Beach	Low	Low	Med	−1.47–5.54	0.01–14.70	−0.79–1.07	1.00–1.04	111.97	4.80	48.05–99.29	0.17	0.93
Ft Lauderdale Beach	Low	Low	Low	−1.58–6.35	0.14–25.32	−3.90–3.09	1.00–1.14	111.67	10.50	26.76–142.40	0.14	0.93
Golden Beach	Low	Low	Low	−0.66–6.39	0.01–28.77	−1.36–2.68	1.00–1.20	160.96	1.97	44.54–71.62	0.07	0.33
Gulfstream	Low	Med	Med	−2.06–5.20	0.00–22.41	−1.17–3.5	1.00–1.19	101.47	2.71	15.83–56.60	0.12	0.98
Gulfstream Park	Med	Low	None	−1.04–3.17	1.95–32.38	−1.12–0.23	1.00–1.01	97.93	0.13	33.47–38.00	0.15	0.99
Highland Beach	Med	Med	Med	−1.45–5.77	0.00–52.24	−6.42–2.38	1.00–1.08	98.12	4.62	20.34–74.68	0.08	0.99
Hobe Sound NWR	High	Med	High	−1.94–5.95	0.02–32.54	−1.13–1.91	1.00–1.05	72.51	5.30	28.51–55.99	−0.35	0.95
Hollywood/Hallandale Beach	Low	Low	Low	−0.75–7.12	0.01–15.71	−3.91–3.97	1.00–1.38	114.74	9.30	30.68–86.94	0.11	0.91
John U. Lloyd Beach State Park	Low	Low	Low	−0.76–4.92	0.02–16.80	−1.47–2.40	1.00–1.06	147.58	3.70	40.45–111.6	0.13	0.54
Jupiter Island	High	Med	High	−2.54–9.63	0.00–39.25	−1.74–5.99	1.00–1.32	92.88	13.61	24.12–97.82	−0.32	1.00
Kreusler Park	Low	Low	High	−1.47–2.00	1.43–11.77	−0.61–0.18	1.00–1.02	87.73	0.50	17.50–36.81	−0.03	1.00
Lake Worth Municipal Beach	Low	None	Low	−1.05–10.20	1.87–45.12	−2.79–7.08	1.00–1.43	94.77	0.40	42.80–46.23	−0.01	1.00
Lantana	Low	Low	Med	−0.10–3.80	0.95–26.64	−1.38–1.46	1.00–1.07	91.79	0.20	31.70–41.73	0.08	1.00
Macarthur State Park	High	High	High	−2.16–3.56	0.06–22.34	−1.53–1.09	1.00–1.06	84.51	2.54	22.68–41.92	−0.20	1.00
Ocean Inlet Park	Low	Low	Low	−1.69–3.84	0.71–15.92	−0.72–1.30	1.00–1.02	135.55	0.19	54.38–62.09	0.25	0.70
Ocean Reef Park	Med	Low	High	−0.57–5.22	0.07–30.98	−0.73–1.99	1.00–1.04	105.62	0.20	31.91–77.52	0.35	0.96
Pompano/Lauderdale-by-the-Sea	Med	Low	Low	−1.76–6.37	0.00–26.40	−4.51–3.50	1.00–1.14	117.91	7.60	53.40–136.30	0.19	0.88
Singer Island	High	High	High	−4.24–12.50	0.00–33.07	−0.92–0.73	1.00–1.25	115.25	3.20	17.87–121.50	−0.06	0.90
Sloan's Curve	High	High	High	−1.58–3.65	0.02–28.23	−2.05–0.67	1.00–1.04	108.73	1.33	33.57–53.23	0.01	0.95

Table 5
Beaches and their assigned rank for each species with offshore variables. Minimum and maximum values are reported for elevation, slope, BPI, and rugosity.

Beach	*C. caretta* use	*C. mydas* use	*D. coriacea* use	Offshore variables					
				Offshore Elevation	Offshore Slope	Offshore BPI	Offshore Rugosity	Sine Offshore Aspect	Shoals Area (km2)
Boca Raton Beaches	Med	Med	Med	−22.18 to −0.11	0.00–16.10	−1.27–1.04	1.00–1.05	0.90	0.47
Deerfield/Hillsboro Beaches	Med	Med	Med	−23.75 to −0.66	0.00–33.37	−1.30–0.97	1.00–1.06	0.79	0
Delray Beach	Low	Low	Med	−26.63 to −0.24	0.00–18.10	−1.94–1.53	1.00–1.09	0.85	0.82
Ft Lauderdale Beach	Low	Low	Low	−12.16–0.05	0.00–16.73	−1.41–2.18	1.00–1.11	0.30	0
Golden Beach	Low	Low	Low	−10.95–0.17	0.00–7.70	−1.60–2.09	1.00–1.13	0.36	0
Gulfstream	Low	Med	Med	−18.05 to −0.10	0.00–6.38	−0.75–0.60	1.00–1.01	0.90	0
Gulfstream Park	Med	Low	None	−15.69 to −0.71	0.00–7.31	−0.77–0.56	1.00–1.01	0.87	0
Highland Beach	Med	Med	Med	−21.92–0.12	0.00–5.92	−1.09–0.81	1.00–1.03	0.94	0
Hobe Sound NWR	High	Med	High	−14.2 to −0.33	0.00–16.40	−1.74–1.94	1.00–1.08	0.66	0.80
Hollywood/Hallandale Beach	Low	Low	Low	−12.85–0.17	0.00–13.40	−4.04–6.84	1.00–1.90	0.48	0
John U. Lloyd Beach State Park	Low	Low	Low	−10.21 to −0.32	0.00–11.70	−3.57–3.03	1.00–1.44	0.47	0
Jupiter Island	High	Med	High	−12.26–1.80	0.00–12.10	−2.24–1.74	1.00–1.18	0.90	0
Kreusler Park	Low	Low	High	−14.53 to −0.88	0.00–5.40	−0.48–0.40	1.00–1.01	0.98	0
Lake Worth Municipal Beach	Low	None	Low	−17.72 to −1.30	0.00–8.62	−1.19–0.69	1.00–1.03	0.98	0
Lantana	Low	Low	Med	−13.95 to −0.97	0.01–4.61	−0.48–0.44	1.00–1.01	0.93	0
Macarthur State Park	High	High	High	−13.45 to −0.16	0.00–11.3	−1.29–1.18	1.00–1.05	0.94	0
Ocean Inlet Park	Low	Low	Low	−16.29 to −0.40	0.02–7.61	−0.92–0.53	1.00–1.01	0.96	0
Ocean Reef Park	Med	Low	High	−18.89–0.27	0.00–11.70	−1.07–1.34	1.00–1.07	0.80	0
Pompano/Lauderdale-by-the-Sea	Med	Low	Low	−18.64–0.12	0.00–26.80	−2.16–3.12	1.00–1.23	0.53	0.28
Singer Island	High	High	High	−20.94 to −0.98	0.00–14.10	−0.91–1.02	1.00–1.11	0.95	0
Sloan's Curve	High	High	High	−14.43 to −0.76	0.00–9.52	−0.84–0.75	1.00–1.03	0.97	0

contained similar means for each of the variables tested. This result is not surprising, as there is overlap between many of the highest ranking beaches.

The range of values present on nesting beaches for each species was compared for elevation, slope, TPI/BPI, rugosity, length, width, orientation, and aspect to establish minimum and maximum suitability values. Because most of the nesting beaches were used by all three species, the ranges are similar, with a few exceptions (Table 6).

Two beaches recorded no use by a turtle species for the time period included in this study: Lake Worth Municipal Beach had no recorded nesting *C. mydas*, and Gulfstream Park had no recorded nesting *D. coriacea*. The variables for these two beaches were compared to the extremes of the beaches currently used by the species. Lake Worth Municipal Beach contained onshore TPI and rugosity values beyond the maximum values of nesting beaches, while offshore values were within the ranges of nesting beaches (Table 7).

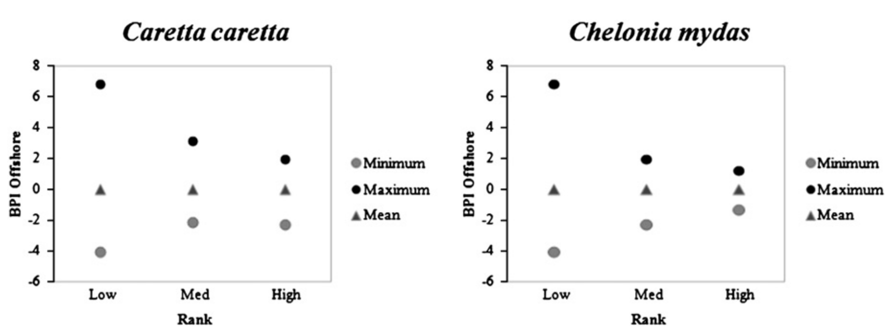

Fig. 4. BPI offshore measurements (minimum, maximum, and mean BPI offshore) for *Caretta caretta* and *Chelonia mydas*.

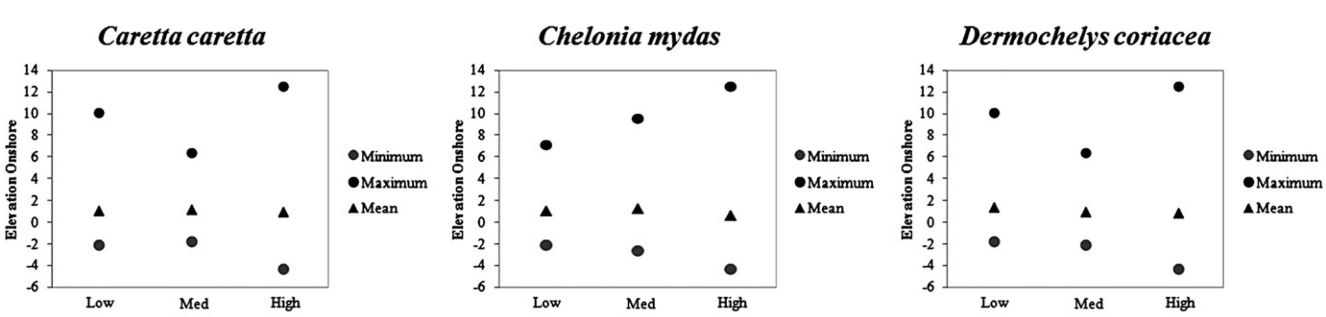

Fig. 5. Elevation onshore measurements (minimum, maximum, and mean elevation onshore) for each of the three species.

Table 6
Onshore and offshore minimums and maximums observed for each variable across species. Note all species use the same ranges, with exceptions noted with [a].

Onshore							
Elevation (m)	Slope	TPI	Rugosity	Length (km)	Width (km)	Sine orientation	Sine aspect
−4.24–12.50	0–52.24	−6.42–7.08[a]	1.00–1.43[a]	0.13–13.61[a]	0.02–0.14	−0.35–0.35	0.33–1.00

Offshore				
Elevation (m)	Slope	BPI	Rugosity	Sine aspect
−26.63–1.80	0–33.37	−4.04–6.84	1.00–1.90	0.36–0.98

[a] The range for *Chelonia mydas* for TPI is −6.42–5.99, and for rugosity it is 1.00–1.38. The range for *Dermochelys coriacea* for beach length is 0.20–13.61 km.

Table 7
Onshore and offshore minimums and maximums compared between nesting beaches of *Chelonia mydas* and Lake Worth Municipal Beach. Variables outside the extremes of nesting beaches are shown in bold.

Onshore								
	Elevation (m)	Slope	TPI	Rugosity	Length (km)	Width (km)	Sine orientation	Sine aspect
Lake Worth	−1.05–10.15	1.87–45.12	**−2.79–7.08**	**1.00–1.43**	0.40	0.04–0.05	−0.01	0.997

Offshore					
	Elevation (m)	Slope	BPI	Rugosity	Sine aspect
Lake Worth	−17.72 to −1.34	0–8.62	−1.19–0.69	1.00–1.03	0.98

Table 8
Onshore and offshore minimums and maximums compared between nesting beaches of *Dermochelys coriacea* and Gulfstream Park. Variables outside the extremes of nesting beaches are shown in bold.

Onshore								
	Elevation (m)	Slope	TPI	Rugosity	Length (km)	Width (km)	Sine orientation	Sine aspect
Gulfstream Park	−1.04–3.17	1.95–32.38	−1.12–0.23	1.00–1.01	**0.13**	0.03–0.04	0.15	0.99

Offshore					
	Elevation (m)	Slope	BPI	Rugosity	Sine aspect
Gulfstream Park	−15.69 to −0.71	0–7.31	−0.77–0.56	1.00–1.01	0.87

The length of Gulfstream Park is below the extremes observed in nesting beaches for *D. coriacea* for period of the nesting years studied, while offshore values were within the ranges of nesting beaches (Table 8). Although the maximum offshore BPI for Gulfstream Park is on the lower end of the observed values, it is still within the range.

3.2. Developing predictive models for nesting density per species

Variables that were highly correlated (Pearson correlation coefficient > 0.8) were removed before model creation: onshore standard deviation of elevation which correlated with onshore maximum elevation; offshore minimum elevation which correlated with offshore average elevation; offshore standard deviation of elevation which correlated with offshore average elevation; offshore maximum rugosity with offshore maximum BPI; and onshore maximum rugosity with onshore maximum TPI. Because the pairs were so highly correlated and also so interrelated, an argument could be made for retention of either variable. For this study, the maximum and average elevations were chosen to be retained over minimum and standard deviation, and maximum BPI/TPI measures were chosen instead of maximum rugosity values. The residuals for all models were randomly scattered above and below the y = 0 line.

Table 9
Multivariate stepwise linear regression results. All beta weights are significant at $p<0.05$, except for maximum onshore TPI in the *Caretta caretta* model, which is significant at $p<0.1$. SE = standard error; VIF = variance inflation factor.

Response	Model adjusted R^2	Variable	Parameter estimate	SE	Cumulative R^2 values	Beta weights	VIF
Caretta caretta	0.63	Intercept	57.83	36.46			
		SineOrient	−48.90	20.05	0.51	−0.39	1.28
		OnMinEle	−326.02	99.50	0.63	−0.53	1.28
Chelonia mydas	0.49	Intercept	8.95	7.20			
		TPIOnMax	−2.65	1.39	0.07	−0.32	1.07
		OnMinEle	−6.81	3.22	0.43	−0.39	1.33
		OffMaxEle	−37.00	16.22	0.56	−0.43	1.37
Dermochelys coriacea	0.47	Intercept	4.22	0.69			
		SineOrient	−9.89	2.38	0.38	−0.69	1.03
		TPIOnMax	−0.52	0.23	0.52	−0.37	1.03

For *C. caretta*, transformed orientation (SineOrient) and minimum onshore elevation (OnMinEle) were able to model nesting density (adjusted $R^2 = 0.63$) (Table 9). The beta weights (standardized multiple regression coefficients) were similar, with the onshore minimum elevation as the most influential predictor variable as identified by the beta weight.

For *C. mydas*, nesting density was modeled with onshore minimum elevation (OnMinEle), onshore maximum TPI (TPIOnMax), and offshore maximum elevation (OffMaxEle) (adjusted $R^2 = 0.49$) (Table 9). Offshore maximum elevation was the most relatively important predictor variable, with offshore maximum TPI as the least.

For *D. coriacea*, transformed orientation (SineOrient) and maximum onshore TPI (TPIOnMax) were able to model nesting density (adjusted $R^2 = 0.47$) (Table 9). The beta weights showed orientation influencing the model more than the maximum onshore TPI.

4. Discussion

The relationships between geomorphological information and sea turtle nesting beaches have been largely restricted to a handful of beaches at a time, due to time and financial constraints. Multiple species and beach comparisons have been limited and infrequent. The ability to compare more than twenty beaches across three species provides new insights to sea turtle nesting beaches for elevation-derived characteristics, especially in regard to identifying preferred ranges for different morphological features and modeling nesting densities.

Sea turtles can use beaches with a wide range of acceptable values, and these ranges overlap for the different species. However, it appears that species have limits to their accepted variable ranges, and beaches that fall outside of these limits are not used for nesting activities. The ranges of values observed on nesting beaches for the different species should be compared to other nesting areas to determine if such values can be applied elsewhere. These ranges may also help determine how beach-altering activities, such as sand mining or hurricanes, will affect nesting densities in subsequent years.

Sea turtle nesting activity can be successfully modeled with a small number of topographical variables, despite overall beach similarities. Therefore, as Provancha and Ehrhart (1987) and Mortimer (1982) suggested, beach characteristics, as opposed to sand characteristics, may be important factors in determining why sea turtles nest on some beaches more often than on others.

In addition, although bathymetric details have been suggested as possibly influencing nesting activity (Mortimer, 1982; Provancha & Ehrhart, 1987) the results from this study indicate that onshore characteristics are more influential for predicting nest density, given the variables tested. Measures of TPI, in particular, were present in all three models, demonstrating that the difference in slope of an area from the neighboring regions influences nesting activity for the three species.

Because Florida contains one of the largest *C. caretta* rookeries in the world and one of the largest nesting areas in the Atlantic for *C. mydas* (Meylan et al., 1995), the ability to successfully model nesting density may also be repeatable with other rookeries elsewhere in these species' ranges. Although the beaches in Florida provide the only continuously used nesting area in the continental United States for *D. coriacea* (Meylan et al., 1995), it is unclear if using other more important nesting areas may provide different models, as these areas can support larger numbers of nesting females and may therefore show potentially different results.

The beaches included in this study have relatively narrow elevation ranges, and the inability to capture fine morphological details due to the limitations of spatial resolution may result in the loss of potentially important information. Because of the overall similarities between the beaches, ranges for variables often overlap between beaches used by different species, and each species does not appear to prefer one extreme of the range over another. However, beaches whose ranges fall outside the established ranges are not used for nesting (e.g. Gulfstream Park for *D. coriacea*), and the small differences present can be used to model beach use. Another potential shortcoming is the timing of the LiDAR flight collection. Although the data were collected at low tide, but not at absolute low tide, some low-lying areas may not have been included in the designated onshore areas.

Elevation and elevation-based morphological details are not the only determining factors for beach use by sea turtles. Vegetation, beach use by humans including construction and beach traffic, and presence of predators are other possible influences to sea turtle nesting activity. However, the results from this study illustrate that beach physical characteristics can be used to predict beach use by nesting female sea turtles.

The use of highly detailed topographical and bathymetrical data enables researchers to quickly and efficiently compare multiple study areas at once, as well as providing insights about geomorphological nuances that were not previously possible with traditional field methods, particularly in comparison to transect-based studies. LiDAR can be used to further refine known habitat requirements for species. In addition, this work highlights the potential of LiDAR to model and potentially predict habitat use for species for which coastal morphology is an important characteristic. The methods and results from this study can be applied to other species for which elevation and morphological characteristics are a limiting factor to a species' distribution. The increased spatial resolution of LiDAR, and potentially high temporal frequency (i.e. dependent on aircraft and not satellite), allow for new research focuses for wildlife, and for those species that utilize areas susceptible to sea level rise, the need for more complete knowledge of habitat suitability requirements is of increasing importance.

References

Austin, M. P., Nicholls, A. O., & Margules, C. R. (1990). Measurement of the realized qualitative niche — Environmental niches of 5 eucalyptus species. *Ecological Monographs*, *60*, 161–177.

Brown, L., & Macdonald, D. W. (1995). Predation on green turtle *Chelonia mydas* nests by wild canids at Akyatan beach, Turkey. *Biological Conservation*, *71*, 55–60.

Buhl-Mortensen, P., Dolan, M., & Buhl-Mortensen, L. (2009). Prediction of benthic biotopes on a Norwegian offshore bank using a combination of multivariate analysis and GIS classification. *ICES Journal of Marine Science*, *66*, 2026–2032.

Bustard, H. R. (1972). *Sea turtles: Natural history and conservation.* New York, New York: Taplinger Publishing Company.

Bustard, H. R., & Greenham, P. (1968). Physical and chemical factors affecting hatching in green sea turtle *Chelonia Mydas* (L). *Ecology*, *49*, 269–276.

Chen, H. C., Cheng, I. J., & Hong, E. (2007). The influence of the beach environment on the digging success and nest site distribution of the green turtle, *Chelonia mydas*, on Wan-an Island, Penghu Archipelago, Taiwan. *Journal of Coastal Research*, *23*, 1277–1286.

Collin, A., Archambault, P., & Long, B. (2008). Mapping the shallow water seabed habitat with the SHOALS. *IEEE Transactions on Geoscience and Remote Sensing*, *46*, 2947–2955.

De Stoppelaire, G. H., Gillespie, T. W., Brock, J. C., & Tobin, G. A. (2004). Use of remote sensing techniques to determine the effects of grazing on vegetation cover and dune elevation at Assateague Island National Seashore: Impact of horses. *Environmental Management*, *34*, 642–649.

Fish and Wildlife Research Institute, F.F.a.W.C.C (2008). *Reported sea turtle nesting activity in Florida, 1993–2007* In.

Gesch, D. B. (2009). Analysis of Lidar elevation data for improved identification and delineation of lands vulnerable to sea-level rise. *Journal of Coastal Research*, *25*, 49–58.

Horrocks, J. A., & Scott, N. M. (1991). Nest site location and nest success in the hawksbill turtle (*Eretmochelys imbricata*) in Barbados, West Indies. *Marine Ecology Progress Series*, *69*, 1–8.

Iampietro, P., & Kvitek, R. (2002). Quantitative seafloor habitat classification using GIS terrain analysis: Effects of data density, resolution, and scale. *Proceedings of the 22nd Annual ESRI User Conference. San Diego, CA* (pp. 8–12).

Iampietro, P. J., Young, M. A., & Kvitek, R. G. (2008). Multivariate prediction of rockfish habitat suitability in Cordell Bank National Marine Sanctuary and Del Monte shalebeds, California, USA. *Marine Geodesy*, *31*, 359–371.

Jenks, G. F. (1967). The data model concept in statistical mapping. *International Yearbook of Cartography*, *7*, 186–190.

Jenness, J. (2011). DEM surface tools for ArcGIS (surface_area.exe) v. 2.1.292. In http://www.jennessent.com/arcgis/surface_area.htm Last accessed 7 December 2011.

Long, T. M., Angelo, J., & Weishampel, J. F. (2011). LiDAR-derived measures of hurricane- and restoration-generated beach morphodynamics in relation to sea turtle nesting behaviour. *International Journal of Remote Sensing*, *32*, 231–241.

Lundblad, E. R., Wright, D. J., Miller, J., Larkin, E. M., Rinehart, R., Naar, D. F., et al. (2006). A benthic terrain classification scheme for American Samoa. *Marine Geodesy*, *29*, 89–111.

Majka, D., Jenness, J., & Beier, P. (2007). *CorridorDesigner: ArcGIS tools for designing and evaluating corridors.* Available at http://corridordesign.org.

Meylan, A., Schroeder, B., & Mosier, A. (1995). *Sea turtle nesting activity in the State of Florida 1979–1992. St. Petersburg, Florida.*

Mortimer, J. A. (1982). Factors influencing beach selection by nesting sea turtles. In K. A. Bjorndal (Ed.), *Biology and conservation of sea turtles* (pp. 45–51). Washington, DC: Smithsonian Institution Press Pages.

Mortimer, J. A. (1990). The influence of beach sand characteristics on the nesting-behavior and clutch survival of green turtles (*Chelonia mydas*). *Copeia*, 802–817.

Parson, L. E., Lillycrop, W. J., Klein, C. J., Ives, R. C. P., & Orlando, S. P. (1997). Use of lidar technology for collecting shallow water bathymetry of Florida Bay. *Journal of Coastal Research*, *13*, 1173–1180.

Piedallu, C., & Gegout, J. (2008). Efficient assessment of topographic solar radiation to improve plant distribution models. *Agricultural and Forest Meteorology*, *148*, 1696–1706.

Pierce, K. B., Lookingbill, T., & Urban, D. (2005). A simple method for estimating potential relative radiation (PRR) for landscape-scale vegetation analysis. *Landscape Ecology*, *20*, 137–147.

Provancha, J. A., & Ehrhart, L. M. (1987). Sea nesting trends at John F. Kennedy Space Center and Cape Canaveral Air Force Station, Florida, and relationships with factors influencing nest site selection. *Ecology of east Florida sea turtles.* In W. N. Witzell (Ed.), *NOAA Tech. Rept. NMFS*, *53*. (pp. 33–44).

Quadros, N. D., Collier, P. A., & Fraser, C. S. (2008). Integration of bathymetric and topographic Lidar: A preliminary investigation. *The International Archives of the Photogrammetry, Remote Sensing and Spatial Information Sciences*, *B8*, 1299–1304.

St Johns River Water Management District, SJRWMD (SJRWMD, 2000). GIS Download Library. In http://www.sjrwmd.com/gisdevelopment/docs/themes.html Last accessed 7 December 2011.

Stancyk, S. E., & Ross, J. P. (1978). Analysis of sand from green turtle nesting beaches on Ascension Island. *Copeia*, 93–99.

Stockdon, H. F., Doran, K. S., & Sallenger, A. H. (2009). Extraction of lidar-based dune-crest elevations for use in examining the vulnerability of beaches to inundation during hurricanes. *Journal of Coastal Research*, *25*, 59–65.

Streutker, D. R., & Glenn, N. F. (2006). LiDAR measurement of sagebrush steppe vegetation heights. *Remote Sensing of Environment*, *102*, 135–145.

Sylvester, C. (2011). Collaboration and Decision Support with PDF: USACE National Coastal Mapping Program Examples, Spatial Data Brach, USACE Mobile District, Joint Airborne Lidar Bathymetry Technical Center of Expertise. In http://www.usace-isc.org/presentation/HHC-Misc/Collaboration%20and%20Decision%20Support%20with%20PDF_C.%20Sylvester.pdf Last accessed 7 April 2012.

Wedding, L., Friedlander, A., Mcgranaghan, M., Yost, R., & Monaco, M. (2008). Using bathymetric lidar to define nearshore benthic habitat complexity: Implications for management of reef fish assemblages in Hawaii. *Remote Sensing of Environment*, *112*, 4159–4165.

Weiss, A. (2001). Topographic position and landforms analysis. *Poster presentation, ESRI User Conference, San Diego, CA* pp. 200-200.

Whitmore, C. P., & Dutton, P. H. (1985). Infertility, embryonic mortality and nest-site selection in leatherback and green sea turtles in Suriname. *Biological Conservation*, *34*, 251–272.

Wilson, M. F. J., O'Connell, B., Brown, C., Guinan, J. C., & Grehan, A. J. (2007). Multiscale terrain analysis of multibeam bathymetry data for habitat mapping on the continental slope. *Marine Geodesy*, *30*, 3–35.

Zawada, D. G., & Brock, J. C. (2009). A multiscale analysis of coral reef topographic complexity using lidar-derived bathymetry. *Journal of Coastal Research*, *25*, 6–15.